ACS APPLIED MATERIALS & INTERFACES

Research Article

Cite This: ACS Appl. Mater. Interfaces 2018, 10, 37829−37834

www.acsami.org

Multivalent Antibody−Nanoparticle Conjugates To Enhance the Sensitivity of Surface-Enhanced Raman Scattering-Based Immunoassays

Miyeon Lee,[†,⊥] Hyeran Kim,[‡,⊥] Eungwang Kim,[†] So Yeon Yi,[§] Seul Gee Hwang,[‡,∥] Siyeong Yang,[†] Eun-Kyung Lim,[‡,∥] Bongsoo Kim,*[,†] Juyeon Jung,*[,‡,∥] and Taejoon Kang*[,‡,∥]

[†]Department of Chemistry, KAIST, Daejeon 34141, Korea

[‡]Hazards Monitoring Bionano Research Center and [§]BioNano Health Guard Research Center, KRIBB, Daejeon 34141, Korea

[∥]Department of Nanobiotechnology, KRIBB School of Biotechnology, UST, Daejeon 34113, Korea

Supporting Information

ABSTRACT: Multivalent immunoprobes can improve the sensitivity of biosensors because increased valency can strengthen the binding affinity between the receptor and target biomolecules. Here, we report surface-enhanced Raman scattering (SERS)-based immunoassays using multivalent antibody-conjugated nanoparticles (NPs) for the first time. Multivalent antibodies were generated through the ligation of Fab fragments fused with Fc-binding peptides to immunoglobulin G. This fabrication method is easy and fast because of the elimination of heterologous protein expression, high degrees of antibody modifications, and covalent chemical ligation steps. We constructed multivalent antibody−NP conjugates (MANCs) and employed them as SERS immunoprobes. MANCs improved the sensitivity of SERS-based immunoassays by 100 times compared to standard antibody−NP conjugates. MANCs will increase the feasibility of practical SERS-based immunoassays.

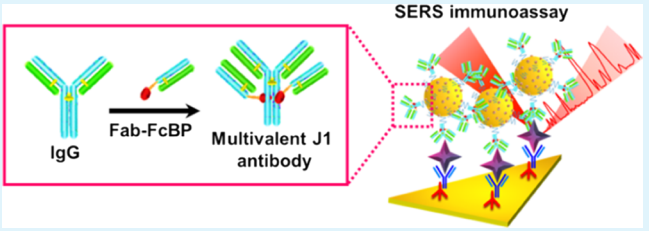

KEYWORDS: *multivalent antibody, antibody−nanoparticle conjugate, surface-enhanced Raman scattering, immunoassay, biosensor*

1. INTRODUCTION

Immunoassays are one of the most commonly used rapid and sensitive analytical methods for the detection and quantification of biomolecules in a wide range of fields, including disease diagnosis, food safety, and environmental monitoring.[1] Recent immunoassays have employed various types of readout signals, including color change, surface plasmon resonance (SPR),[2] fluorescence,[3] electrochemistry,[4] and surface-enhanced Raman scattering (SERS),[5] advancing into sophisticated analyte detection methods. Among various types of immunoassays, SERS-based immunoassays have attracted much attention because of their single-molecule sensitivity, photostability, and excellent multidetection capability.[6] SERS is a phenomenon that significantly increases the Raman signals of molecules near metallic nanostructures (hot spots). Typical SERS-based immunoassays detect molecules through the assemblies of immune substrates and SERS immunoprobes. The immune substrates capture specific analytes from a sample. The SERS immunoprobes recognize the analytes captured on the immune substrates and provide SERS signals. Therefore, SERS immunoprobes are critical for the sensitive and quantitative detection of analytes. During two decades, several SERS immunoprobes have been developed for the improvement of SERS enhancement, chemical or physical stability, and multiplex sensing ability. For example, Cheng et al. reported antibody-conjugated SERS nanotags for the accurate diagnosis of prostate cancer.[7] Guerrini et al. reported that Ag nanoparticles (NPs) coated with spermine can be used for gaining genomic information on DNA duplexes.[8] Kim et al. demonstrated dealloyed intra-nanogap particles with highly robust and quantifiable SERS signals.[9] Wang et al. developed Au NPs decorated with a specific aptamer and a Raman reporter for the multidetection of cancerous exosomes.[10]

Multivalency between two or more combined biomolecules plays an important role in many biological actions by providing a strong binding affinity.[11] In biosensing, the use of multivalency can be highly advantageous because the increased valency can increase the binding affinity between the receptor and target molecules up to tens of times, improving the biosensor sensitivity.[12] Moreover, it has been recently demonstrated that multivalent bioreceptors enable the more selective detection of target molecules.[13,14] Consequently, SERS-based immunoassays adopting multivalency could exhibit maximized sensitivity and selectivity for analytes, bringing us one step closer to the practical applications of SERS-based immunoassays. However, as SERS-based immunoassays using multivalent antibodies have

Received: August 3, 2018
Accepted: October 16, 2018
Published: October 16, 2018

DOI: 10.1021/acsami.8b13180
ACS Appl. Mater. Interfaces 2018, 10, 37829−37834

not yet been implemented, we developed a multivalent antibody-conjugated NP as a novel SERS immunoprobe.

For the application of multivalency in immunoassays, it is a priority to produce multivalent receptors with increased target-binding affinity in a simple mass-produced manner. We constructed a multivalent antibody simply by attaching Fab fragments fused with Fc-binding peptides (Fab−FcBP) to the Fc region of immunoglobulin G (IgG). This method makes it possible to prepare multivalent antibodies routinely without the loss of antibody activity because complicated fusion protein expression steps and chemical ligation processes are not required. We produced a multivalent antibody against Jagged1 (J1) and evaluated the binding property of the multivalent antibody against the antigen. Furthermore, we fabricated multivalent antibody−NP conjugates (MANCs) and employed them as SERS immunoprobes for the first time. Importantly, J1 was detectable at a low concentration of 10 pM using MANCs. This limit of detection (LOD) is 100 times lower than that of standard J1 antibody−NP conjugates (SANCs). We expect that various types of multivalent antibodies will be generated and corresponding types of MANCs will be developed. Therefore, SERS-based immunoassays using MANCs might be used in the real world for disease diagnosis, environmental monitoring, and biochemical analysis.

2. RESULTS AND DISCUSSION

Multivalent antibodies bind to multiple sites on one target, which may result in higher functional affinity and avidity over their monomeric forms depending on the number of binding sites.[15−18] Multimeric forms of antibodies are produced by genetic engineering, hybrid hybridomas, or chemical conjugation, and they have been extensively tested for use as therapeutic agents and in tumor diagnostics.[19−21] However, production of multivalent antibody by genetic engineering or hybrid hybridomas method has been found too low in yield and labor-intensive. The chemical conjugation of two or more antibodies or antibody fragments is also ineffective and can severely impair antibody activity. Hence, a new approach is needed to produce multivalent antibodies without complicated processes and without compromising the activity of the antibody. Here, we present an easy and fast way to produce multivalent antibodies that eliminate the need for heterologous expression and fusion of antibodies or chemical modifications, facilitating the production of multivalent antibodies without the loss of antibody activity. Figure 1a shows a schematic representation of the multivalent antibody production. The Fab fragment is a region of the antibody that retains its antigen-binding activity but lacks the Fc portion of IgG. For the preparation of a multivalent antibody, we designed and expressed Fab−FcBP. The generation of Fab−FcBP makes it possible to easily produce a multivalent antibody because FcBP can simply bind to the Fc region of IgG. As shown in Figure 1a, a multivalent antibody is producible by the ligation of Fab−FcBP to the Fc region of IgG.

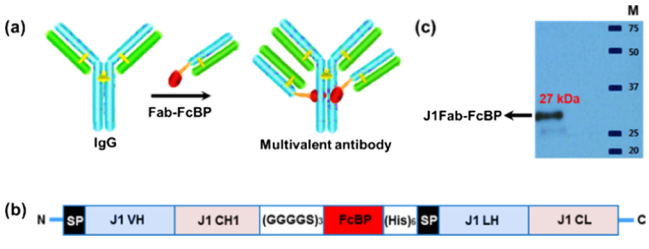

Figure 1. (a) Schematic representation of multivalent antibody production. Fab−FcBP is ligated to the Fc region of IgG to generate a multivalent antibody. (b) Schematic diagram of the phagemid vector in which the Fab fragment of the J1 monoclonal antibody is cloned. (c) Western blot analysis of J1Fab−FcBP.

As a proof of concept, we tried to generate a multivalent antibody capable of efficiently detecting J1. Because over-expression of the Notch ligand J1 is associated with increased progression, metastasis and recurrence of prostate cancer, breast cancer, glioma, and head and neck cancers, a specific antibody against J1 is expected to be used in the diagnosis of cancer-related Notch signaling overexpression.[22,23] In addition, the J1 antibody can be used as a therapeutic agent by blocking the binding of J1 to the Notch receptor.[24] We employed a Fab fragment derived from the J1 monoclonal antibody, which was found in the phage display antibody library. A J1Fab−FcBP fusion gene was synthesized using a secretion signal peptide, J1 VH-CH, a (GGGGS)3 linker, a codon-optimized FcBP (DCAWHLGELVWCT), a His tag, a secretion signal peptide, and J1 VL-CL, cloned into a pKB-Fab100 vector, and expressed in the *Escherichia coli* strain TG1 via induction with 1 mM, isopropyl-1-thio-β-D-galactopyranoside at 30 °C overnight (Figure 1b). The cells were pelleted and resuspended in periplasmic extraction buffer containing 0.2 M Tris-HCl, 0.5 mM ethylenediaminetetraacetic acid, and 0.5 mM sucrose at pH 8.0. After centrifugation, soluble J1Fab−FcBP fragments from the supernatant were purified using protein L resin. The J1Fab−FcBP fusion protein was detected at its predicted size of 27 kDa by western blotting (Figure 1c). The purified J1Fab−FcBP was reacted with the J1 antibody at room temperature, and the formation of J1Fab−FcBP and the J1 antibody complex (multivalent J1 antibody) was confirmed by western blotting (Figure S1).

To examine the antigen-binding ability of the multivalent J1 antibody, an SPR sensor chip with an immobilized J1 peptide was reacted with the multivalent J1 antibody, standard J1 antibody, and IgG. As shown in Figure 2a, J1 peptide (0.5 mg/mL) was immobilized at the 250 RU level on the chip surface and blocked with amine-PEG (1 mg/mL); then, the multivalent J1 antibody, standard J1 antibody, or IgG was flowed over the J1 peptide-coated chip. The binding ability of the multivalent J1 antibody to the J1 peptide was approximately twofold more efficient than that of the J1 antibody. In addition, when the concentration of the multivalent J1 antibody was increased to 0.1, 0.2, 0.4, 0.6, and 0.8 μM, the RU values of SPR for the J1 peptide increased to 70, 160, 300, 538, and 669 RU, respectively (Figure 2b). These data clearly confirm that the multivalent J1 antibody, which contains four antigen-binding sites, has significantly enhanced binding avidity compared with the conventional antibody.

The multivalent J1 antibody developed herein can be effectively applied to sensor systems that require improved binding activity because it is efficiently immobilized by interacting with the immobilized antigen on the surface of the sensor. The binding ability of the multivalent J1 antibody to the J1 peptide on various solid surfaces was explored. First, the multivalent J1 antibody (0.1 mg/mL) or J1 antibody (0.1 mg/mL) was immobilized on a Au chip, and the J1 peptide was flowed over the chip at various concentrations (50 000, 5000, 500, 50, 5, and 0.5 ng/mL) and analyzed using SPR imaging (Figure S2a). The signal of the multivalent J1 antibody that reacted with the J1 peptide at the surface was brighter than that of the J1 antibody, indicating that the multivalent J1 antibody

DOI: 10.1021/acsami.8b13180
ACS Appl. Mater. Interfaces 2018, 10, 37829−37834

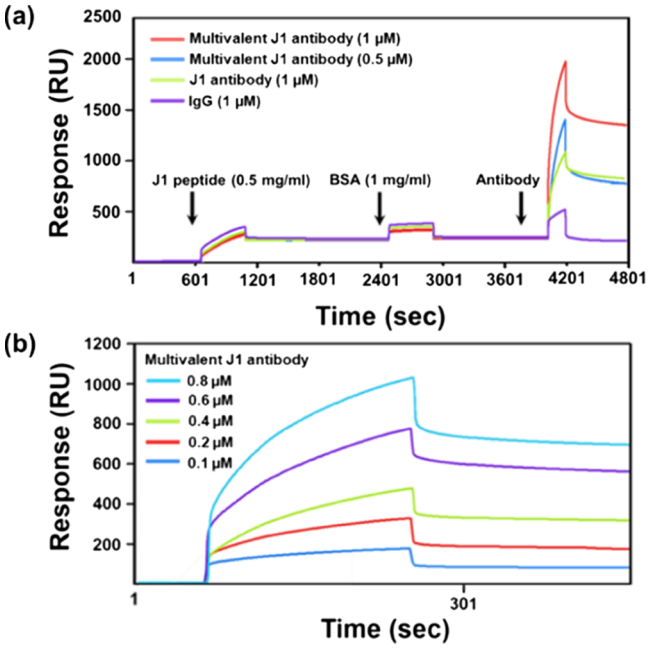

Figure 2. (a) Antigen-binding abilities of the multivalent J1 antibody (0.5 and 1 μM), standard J1 antibody (1 μM), and IgG (1 μM) using J1 peptide-coated SPR chips. RU values were obtained from three independent experiments. (b) Antigen-binding ability of the multivalent J1 antibody (0.1, 0.2, 0.4, 0.6, and 0.8 μM) using J1 peptide-coated SPR chips.

has higher binding affinity to the J1 peptide than the J1 antibody. Second, we compared the binding capacity of the multivalent J1 antibody or J1 antibody to J1 peptide using the dot blot method. The multivalent J1 antibody and J1 antibody were added to the nitrocellulose membrane, and Cy5-labeled J1 peptide (1 μg/mL) was reacted; the degree of fluorescence at 635 nm was then detected. The multivalent J1 antibody showed an intensity at 1 nM similar to that at 100 nM of the J1 antibody, indicating that the sensitivity of the multivalent J1 antibody increased by approximately 100-fold (Figure S2b). Third, a glass surface was covered with the J1 peptide (1 mg/mL), and Cy3-labeled multivalent J1 or J1 antibodies were reacted at different concentrations (1000, 500, 250, 100, and 10 μg/mL); fluorescence images were then captured at 532 nm. The multivalent J1 antibody reacted with the J1 peptide even at 0.01 μg/mL, whereas the standard J1 antibody reacted with the J1 peptide at a minimum concentration of 0.1 μg/mL (Figure S2c). Fourth, immunoprecipitation of the multivalent J1 antibody using the J1 peptide revealed that the multivalent J1 antibody reacted more than twice as much as the J1 antibody (Figure S2d). These results demonstrate the wide applicability of multivalent antibodies.

To investigate the SERS-based immunoassay with multivalency, we developed a SERS immunoprobe using a multivalent J1 antibody. Figure 3a shows a schematic illustration of MANC preparation. Au NPs (20 nm) were modified with malachite green isothiocyanate (MGITC), a commonly used Raman reporter that resonantly absorbs light near the wavelength of 633 nm, and then reacted with a thiolated, multivalent J1 antibody. The thiolated antibody was prepared by the amine-based conjugation of the antibody to *N*-hydroxysuccinimidyl-11-mercaptoundecanoate. SANCs were also prepared in the same manner by using the standard J1 antibody instead of the multivalent J1 antibody. As an immune substrate, we adopted a standard J1 antibody-immobilized Au nanoplate. The single-crystalline Au nanoplates were synthesized in the vapor phase as previously reported (Figure S3).[25] Briefly, the Au slug was placed in a horizontal quartz tube furnace system and heated to 1130 °C, maintaining the chamber pressure at 5−15 Torr. Next, the Au vapor was transported to the sapphire substrate where the Au nanoplates were grown. The synthesized Au nanoplates were transferred onto a silicon wafer, and the surfaces of nanoplates were modified by Cys3-protein G and standard J1 antibody sequentially. Because the single-crystalline Au nanoplates have flat and clean surfaces, they allow uniform antibody immobilization and can provide stable and reproducible SERS signals.[25] The Au nanoplates allow uniform antibody immobilization and can provide stable and reproducible SERS signals.[25] The right panel of Figure 3a displays a MANC-on-nanoplate structure

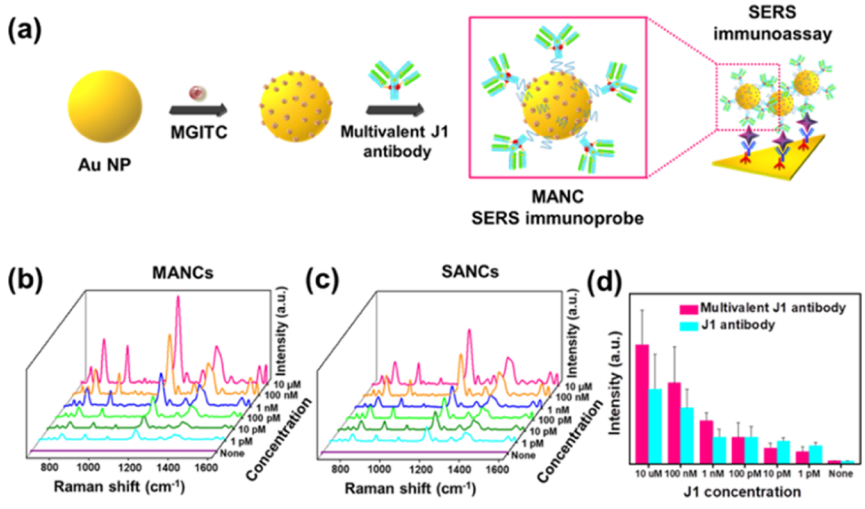

Figure 3. (a) Schematic illustration of MANC preparation for J1 peptide detection. In the presence of J1, MANC-on-nanoplate structures are constructed and SERS signals of MGITC are observed. (b) SERS spectra of MGITC obtained from MANC-on-nanoplate structures by varying the concentration of J1. (c) SERS spectra of MGITC obtained from SANC-on-nanoplate structures with varying J1 concentrations. (d) Plot of band intensity at 1175 cm^{-1} vs the concentration of J1. Magenta and cyan bars were obtained using MANCs and SANCs, respectively. Data represent the mean plus standard deviation of eight measurements.

DOI: 10.1021/acsami.8b13180
ACS Appl. Mater. Interfaces 2018, 10, 37829−37834

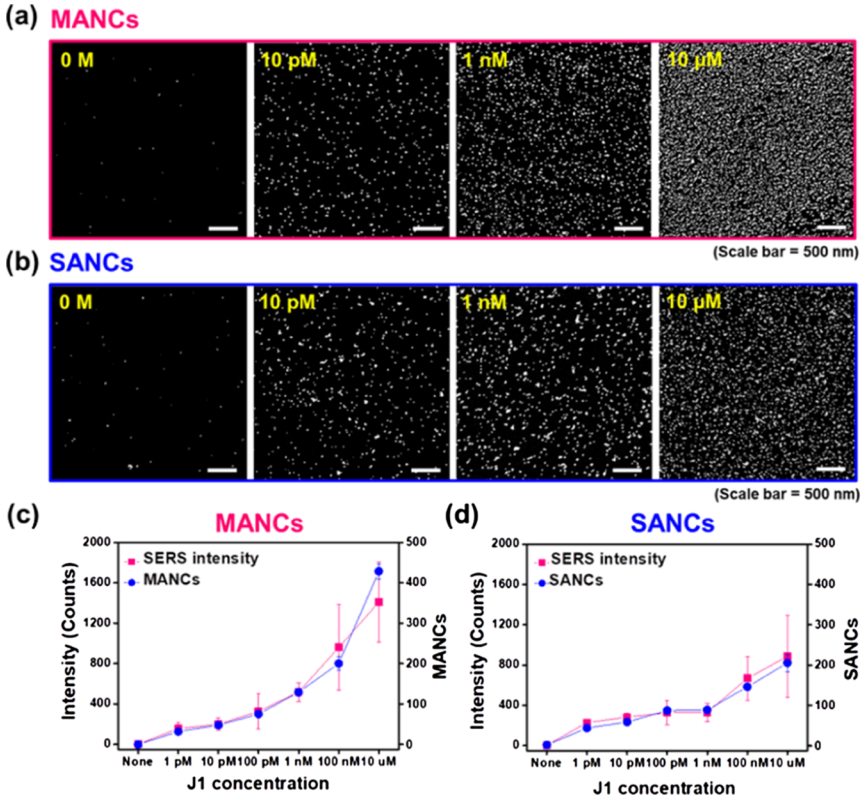

Figure 4. (a) SEM images of MANC-on-nanoplate structures with varying J1 concentrations. (b) SEM images of SANC-on-nanoplate structures with varying J1 concentrations. (c) SERS intensity and number of MANCs on nanoplates (1 μm × 1 μm) as a function of J1 peptide concentration. (d) SERS intensity and number of SANCs on nanoplates (1 μm × 1 μm) as a function of J1 peptide concentration.

after the detection of J1. Only in the presence of J1, can the MANC-on-nanoplate structures be constructed and strong SERS signals of MGITC be observed. The estimated enhancement factor was 3.02 × 10^7. Figure 3b,c shows the results of SERS-based immunoassays for J1 using MANCs and SANCs, respectively. When MANCs were employed, the SERS signals of MGITC gradually increased as the concentration of J1 increased from 10 pM to 10 μM. At a J1 concentration of 1 pM, the SERS signals were distinguishable from those of the blank sample but undistinguishable from those of 10 pM. We estimated the LOD of the SERS-based J1 immunoassay with MANCs to be 10 pM. When SANCs were used, SERS signals increased in the range of J1 concentrations from 1 nM to 10 μM. At a lower concentration of 1 nM, similar spectra were obtained regardless of the J1 concentration. The LOD of SERS-based J1 immunoassay with SANCs is 1 nM. To compare SERS-based immunoassays for J1 using MANCs and SANCs, we plotted the band intensity at 1175 cm^{-1} versus the concentration of J1 (Figure 3d). Because 1175 cm^{-1} band of MGITC is strongest and not overlapped by other peaks, we choose 1175 cm^{-1} band for the calibration of SERS-based immunoassays. Figure 3d clearly indicates that MANCs enhanced the sensitivity of SERS-based immunoassay for J1. Meanwhile, the feeble signals of the blank sample were attributed to the well-immobilized antibody on the ultraflat Au nanoplate. Additionally, we investigated the selectivity of SERS-based immunoassay for J1 (Figure S4). Only in the presence of J peptide, strong SERS signals of MGITC were obtained. We also demonstrated that J1 in 10% serum sample could be detected by using the MANC-on-nanoplate structure (Figure S5). These results indicate that the multivalent J1 antibody has specific binding affinity to J1 peptide.

To explore the SERS-based immunoassay with multivalency in depth, we captured scanning electron microscopy (SEM) images of MANC- and SANC-on-nanoplate structures, respectively, with varying J1 concentrations (Figures 4a,b and S6). When MANCs were used to detect J1, the number of MANCs increased from 10 pM to 10 μM, similar to the SERS-based immunoassay results. Figures 4a and S4 clearly show that MANCs were well attached to the Au nanoplates without aggregation for all J1 peptide concentrations. When SANCs were employed, the number of SANCs increased slightly from 1 nM to 10 μM. At a J1 peptide concentration of 10 μM, MANCs were more densely assembled on the nanoplate than SANCs, indicating that MANCs have a higher binding affinity to the J1 peptide than SANCs. For the quantitative analysis, we compared the SERS intensity and the number of SERS immunoprobes in a unit area (1 μm × 1 μm nanoplate). Figure 4c,d represents plots of the SERS intensity and the number of MANC- or SANC-on-nanoplate structures versus the J1 peptide concentration. The SERS intensity and the number of SERS immunoprobes are well correlated because the SERS signals are obtained from hot spots formed by the SERS immunoprobes. At high J1 concentrations of 10 μM, 100 nM, and 1 nM, the numbers of MANCs were 429, 202, and 131 and the numbers of SANCs were 207, 148, and 91, respectively. At low J1 concentrations of 100, 10, and 1 pM, the numbers of MANCs were 77, 50, and 34 and the numbers of SANCs were 89, 61, and 46, respectively. These results suggest that the high binding affinity of MANCs for J1 could enhance the sensitivity of the SERS-based immunoassay for J1. A single target analyte can be more strongly captured by collective and multiple binding molecules for enhanced target recognition. For many targets and receptors, therefore, enhanced binding

DOI: 10.1021/acsami.8b13180
ACS Appl. Mater. Interfaces 2018, 10, 37829−37834

affinities by multivalency have been used to improve the detection limits of diverse biosensors. Detection limits of antibody-based immunosensors are heavily relying on antibody affinities to target molecules. Because the multivalent J1 antibodies contain four J1 binding sites, the antibodies can interact with J1 with enhanced affinities. This is why the multivalent antibody can enhance the sensitivity of immunoassay. Because this is the first report of SERS-based immunoassays using a multivalent antibody, we expect that various types of multivalent antibody-based SERS immunoprobes will be developed and used for disease diagnosis, environmental monitoring, and biochemical analysis.

3. CONCLUSIONS

We report the production of a multivalent antibody for the J1 peptide by attaching Fab−FcBP to the Fc region of IgG. The multivalent J1 antibody can be easily and efficiently prepared without the loss of antibody activity because this method does not require complicated multivalent antibody expression or chemical modification steps. Moreover, we evaluated the binding of the multivalent antibody to the antigen using SPR, Au chip dot blot, immunoprecipitation, and glass chips. Furthermore, we fabricated MANCs and employed them as a SERS immunoprobe for the first time. The MANCs exhibited a higher binding affinity for the J1 peptide than the SANCs, thus resulting in highly sensitive detection of the target substance. We anticipate that multivalent antibody-conjugated SERS immunoprobes can serve as potential tools for practical sensing and medical diagnostics.

4. EXPERIMENTAL SECTION

4.1. Materials and Instruments. J1 protein, notch-1, notch-3, and thymidine kinase were purchased from Abcam (USA). Cys3-protein G was purchased from MiCoBioMed (Korea). Citrate-stabilized Au NPs (20 nm), BSA, and human serum were purchased from Sigma-Aldrich (USA). MGITC was purchased from Setareh Biotech (USA). *N*-Hydroxysuccinimidyl-11-mercaptoundecanoate (HS−$(CH_2)_{10}$−NHS) was purchased from ProChimia (Poland). SEM images were obtained using a Nova230 system at an accelerating voltage of 15 keV. SERS measurements were carried out using a LabRAM HR system (HORIBA Jobin Yvon). The excitation source was a He−Ne laser operating at λ = 633 nm, and the laser spot was focused on a sample through a 50× objective lens. The SERS signals were recorded with a thermodynamically cooled electron multiplying charge-coupled device (Andor) mounted on a spectrometer with a 1200-groove/mm grating. SPR experiments were performed with carboxyl dextran CM-5 gold chips on a Biacore 3000 device (Biacore AB).

4.2. Preparation of Multivalent J1 Antibody. A J1Fab−FcBP fusion gene coding a secretion signal peptide, J1 VH-CH, a $(GGGGS)_3$ linker, a codon-optimized FcBP (DCAWHLGELVWCT), a His tag, a secretion signal peptide, and J1 VL-C was synthesized. A pKB-Fab100 vector containing J1Fab−FcBP was transformed in the *E. coli* strain TG1 by heat shock, and protein expression was induced with 1 mM isopropyl-1-thio-β-D-galactopyranoside at 30 °C overnight. The cells were harvested and lysed in periplasmic extraction buffer (0.2 M Tris-HCl, 0.5 mM ethylenediaminetetraacetic acid, and 0.5 mM sucrose at pH 8.0). After centrifugation, soluble J1Fab−FcBP fragments from the supernatant were purified using protein L resin (GE Healthcare). The level of expression and purity of the J1Fab−FcBP fusion protein were analyzed by sodium dodecyl sulfate polyacrylamide gel electrophoresis and then by western blotting. The concentration of J1Fab−FcBP was determined by Bradford assay (Bio-Rad). Next, a purified soluble J1Fab−FcBP fragment was ligated to the Fc region of J1 antibody to produce multivalent J1 antibody using 1:3 reaction ratio between J1 antibody and J1Fab−FcBP for 2 h at room temperature. The reaction mixture was then filtered with a centrifugal filter (MWCO 200 kDa, Advantec MFS) to remove any unreacted J1Fab−FcBP fragment and J1 antibody. The formation of multivalent J1 antibody was confirmed by western blotting. The standard J1 antibody was found in the phage display antibody library.

4.3. Preparation of MANCs and SANCs. MGITC (100 μL; 1 μM in ethanol) solution was added to the Au NP solution to make a 1 mL solution, which was incubated for 45 min at room temperature with orbital shaking. Simultaneously, we mixed 10 μL of HS−$(CH_2)_{10}$−NHS solution (10 μM in tetrahydrofuran) and 100 μL of the multivalent J1 antibody solution [100 ng/mL in phosphate-buffered saline (PBS)] for 45 min at room temperature with orbital shaking. Then, 50 μL of this mixture was added to the MIGTC-conjugated Au NP solution, and the final solution was incubated for 45 min at room temperature with orbital shaking. To purify the MANCs from the remaining chemicals, the solution was centrifuged (13 300 rpm for 15 min) and resuspended in 0.1× PBS. SANCs were prepared in the same manner by using standard J1 antibody instead of multivalent J1 antibody.

4.4. Preparation of Immune Substrates Using Au Nanoplates. We synthesized single-crystalline Au nanoplates by using a horizontal hot-wall single-zone furnace with a 1 in. inner-diameter quartz tube. The setup was equipped with pressure and mass-flow controllers. Ar gas was flowed at a rate of 100 sccm, maintaining the chamber pressure at 5−15 Torr. The Au slug, placed in an alumina boat at the center of the heating zone, was heated to 1130 °C, and the vapor was transported to the lower temperature region by the carrier gas, where Au nanoplates were grown on substrates. The epitaxially grown Au nanoplates were transferred onto a silicon wafer by a simple attachment and detachment process. Au nanoplates on the silicon wafer were incubated with 1 mL of 5 nM Cys3-protein G solution in PBS for 12 h at 4 °C. Next, the nanoplates were rinsed three times with 0.1× PBS. The Cys3-protein G-modified Au nanoplates were immersed in 1 mL of 1 nM J1 antibody solution in PBS for 12 h at 4 °C and rinsed three times with 0.1× PBS.

4.5. SERS-Based Immunoassay for J1 Using MANCs and SANCs. J1 protein was diluted in PBS at various concentrations (from 10 μM to 1 pM). The various concentrated J1 peptide solutions (1 mL) were added to the prepared SERS immune substrates and shaken for 6 h at 4 °C. Next, they were rinsed three times with 0.1× PBS, followed by incubation in the prepared MANC or SANC solution (1 mL) for 45 min at room temperature. After washing with distilled water and drying, SERS signals were obtained. The selectivity test and the detection of J1 protein in the serum sample were accomplished in the same manner.

■ ASSOCIATED CONTENT

Supporting Information

The Supporting Information is available free of charge on the ACS Publications website at DOI: 10.1021/acsami.8b13180.

Western blot analysis of standard J1 antibody and multivalent J1 antibody; application of the multivalent J1 antibody to various sensor systems; schematic illustration of the experimental setup for the synthesis of Au nanoplates and SEM image of Au nanoplates on the substrate; selectivity test of SERS-based immunoassay for J1; detection of J1 in serum; and SEM images of MANC-on-nanoplate structures with varying J1 concentrations and SEM images of SANC-on-nanoplate structures with varying J1 concentrations (PDF)

■ AUTHOR INFORMATION

Corresponding Authors

*E-mail: bongsoo@kaist.ac.kr (B.K.).
*E-mail: jjung@kribb.re.kr (J.J.).
*E-mail: kangtaejoon@kribb.re.kr (T.K.).

ORCID

Bongsoo Kim: 0000-0001-5245-4715

DOI: 10.1021/acsami.8b13180
ACS Appl. Mater. Interfaces 2018, 10, 37829−37834

Taejoon Kang: 0000-0002-5387-6458

Author Contributions

⊥These authors contributed equally.

Notes

The authors declare no competing financial interest.

■ ACKNOWLEDGMENTS

This research was supported by the Center for BioNano Health-Guard funded by the Ministry of Science and ICT (MSIT) of Korea as Global Frontier Project (H-GUARD_2013-M3A6B2078950 and H-GUARD_2014M3A6B2060507), the Bio & Medical Technology Development Program of the National Research Foundation (NRF) funded by MSIT of Korea (NRF-2018M3A9E2022821), the First-Mover Program for Accelerating Disruptive Technology Development through the NRF funded by MSIT of Korea (NRF-2018M3C1B9069834), the Technology Program for establishing biocide safety management (no. RE 201804085) from the Korea Environmental Industry & Technology Institute funded by the Korea Ministry of Environment, and KRIBB initiative Research Program.

■ REFERENCES

(1) Wang, Z.; Zong, S.; Wu, L.; Zhu, D.; Cui, Y. SERS-Activated Platforms for Immunoassay: Probes, Encoding Methods, and Applications. *Chem. Rev.* **2017**, *117*, 7910−7963.

(2) Mullett, W. M.; Lai, E. P. C.; Yeung, J. M. Surface Plasmon Resonance-Based Immunoassays. *Methods* **2000**, *22*, 77−91.

(3) Taitt, C. R.; Anderson, G. P.; Ligler, F. S. Evanescent wave fluorescence biosensors: Advances of the last decade. *Biosens. Bioelectron.* **2016**, *76*, 103−112.

(4) Rackus, D. G.; Shamsi, M. H.; Wheeler, A. R. Electrochemistry, biosensors and microfluidics: a convergence of fields. *Chem. Soc. Rev.* **2015**, *44*, 5320−5340.

(5) Lee, J. M.; Hwang, A.; Choi, H.; Jo, Y.; Kim, B.; Kang, T.; Jung, Y. A Multivalent Structure-Specific RNA Binder with Extremely Stable Target Binding but Reduced Interaction with Nonspecific RNAs. *Angew. Chem., Int. Ed.* **2017**, *129*, 16214−16218.

(6) Lee, T.; Wi, J.-S.; Oh, A.; Na, H.-K.; Lee, J.; Lee, K.; Lee, T. G.; Haam, S. Highly robust, uniform and ultra-sensitive surface-enhanced Raman scattering substrates for microRNA detection fabricated by using silver nanostructures grown in gold nanobowls. *Nanoscale* **2018**, *10*, 3680−3687.

(7) Cheng, Z.; Choi, N.; Wang, R.; Lee, S.; Moon, K. C.; Yoon, S.-Y.; Chen, L.; Choo, J. Simultaneous Detection of Dual Prostate Specific Antigens Using Surface-Enhanced Raman Scattering-Based Immunoassay for Accurate Diagnosis of Prostate Cancer. *ACS Nano* **2017**, *11*, 4926−4933.

(8) Guerrini, L.; Krpetić, Z.; van Lierop, D.; Alvarez-Puebla, R. A.; Graham, D. Direct surface-enhanced Raman scattering analysis of DNA duplexes. *Angew. Chem., Int. Ed.* **2015**, *54*, 1144−1148.

(9) Kim, M.; Ko, S. M.; Kim, J.-M.; Son, J.; Lee, C.; Rhim, W.-K.; Nam, J.-M. Dealloyed Intra-Nanogap Particles with Highly Robust, Quantifiable Surface-Enhanced Raman Scattering Signals for Biosensing and Bioimaging Applications. *ACS Cent. Sci.* **2018**, *4*, 277−287.

(10) Wang, Z.; Zong, S.; Wang, Y.; Li, N.; Li, L.; Lu, J.; Wang, Z.; Chen, B.; Cui, Y. Screening and multiple detection of cancer exosomes using an SERS-based method. *Nanoscale* **2018**, *10*, 9053−9062.

(11) Cuesta, A. M.; Sánchez-Martín, D.; Sanz, L.; Bonet, J.; Compte, M.; Kremer, L.; Blanco, F. J.; Oliva, B.; Álvarez-Vallina, L. In Vivo Tumor Targeting and Imaging with Engineered Trivalent Antibody Fragments Containing Collagen-Derived Sequences. *PLoS One* **2009**, *4*, No. e5381.

(12) Wright, D.; Usher, L. Multivalent Binding in the Design of Bioactive Compounds. *Curr. Org. Chem.* **2001**, *5*, 1107−1131.

(13) Knez, K.; Noppe, W.; Geukens, N.; Janssen, K. P. F.; Spasic, D.; Heyligen, J.; Vriens, K.; Thevissen, K.; Cammue, B. P. A.; Petrenko, V.; Ulens, C.; Deckmyn, H.; Lammertyn, J. Affinity Comparison of p3 and p8 Peptide Displaying Bacteriophages Using Surface Plasmon Resonance. *Anal. Chem.* **2013**, *85*, 10075−10082.

(14) Martinez-Veracoechea, F. J.; Frenkel, D. Designing super selectivity in multivalent nano-particle binding. *Proc. Natl. Acad. Sci. U.S.A.* **2011**, *108*, 10963−10968.

(15) Cuesta, A. M.; Sainz-Pastor, N.; Bonet, J.; Oliva, B.; Álvarez-Vallina, L. Multivalent antibodies: when design surpasses evolution. *Trends Biotechnol.* **2010**, *28*, 355−362.

(16) Nuñez-Prado, N.; Compte, M.; Harwood, S.; Álvarez-Méndez, A.; Lykkemark, S.; Sanz, L.; Alvarez-Vallina, L. The coming of age of engineered multivalent antibodies. *Drug Discov. Today* **2015**, *20*, 588−594.

(17) Miller, K.; Meng, G.; Liu, J.; Hurst, A.; Hsei, V.; Wong, W.-L.; Ekert, R.; Lawrence, D.; Sherwood, S.; DeForge, L.; Gaudreault, J.; Keller, G.; Sliwkowski, M.; Ashkenazi, A.; Presta, L. Design, Construction, and In Vitro Analyses of Multivalent Antibodies. *J. Immunol.* **2003**, *170*, 4854−4861.

(18) Rossi, E. A.; Goldenberg, D. M.; Cardillo, T. M.; Stein, R.; Wang, Y.; Chang, C.-H. Novel Designs of Multivalent Anti-CD20 Humanized Antibodies as Improved Lymphoma Therapeutics. *Cancer Res.* **2008**, *68*, 8384−8392.

(19) Lu, D.; Kotanides, H.; Jimenez, X.; Zhou, Q.; Persaud, K.; Bohlen, P.; Witte, L.; Zhu, Z. Acquired antagonistic activity of a bispecific diabody directed against two different epitopes on vascular endothelial growth factor receptor 1. *J. Immunol. Methods* **1999**, *230*, 159−171.

(20) Dan, L.; Xenia, J.; Haifan, Z.; Yan, W.; Peter, B.; Larry, W.; Zhenping, Z. Complete Inhibition of Vascular Endothelial Growth Factor (VEGF) Activities with a Bifunctional Diabody Directed against Both VEGF Kinase Receptors, fms-like Tyrosine Kinase Receptor and Kinase Insert Domain-containing Receptor. *Cancer Res.* **2001**, *61*, 7002−7008.

(21) Lu, D.; Jimenez, X.; Zhang, H.; Bohlen, P.; Witte, L.; Zhu, Z. Fab-scFv fusion protein: an efficient approach to production of bispecific antibody fragments. *J. Immunol. Methods* **2002**, *267*, 213−226.

(22) Reedijk, M.; Odorcic, S.; Chang, L.; Zhang, H.; Miller, N.; McCready, D. R.; Lockwood, G.; Egan, S. E. High-level coexpression of JAG1 and NOTCH1 is observed in human breast cancer and is associated with poor overall survival. *Cancer Res.* **2005**, *65*, 8530−8537.

(23) Santagata, S.; Demichelis, F.; Riva, A.; Varambally, S.; Hofer, M. D.; Kutok, J. L.; Kim, R.; Tang, J.; Montie, J. E.; Chinnaiyan, A. M.; Rubin, M. A.; Aster, J. C. JAGGED1 expression is associated with prostate cancer metastasis and recurrence. *Cancer Res.* **2004**, *64*, 6854−6857.

(24) Wu, Y.; Cain-Hom, C.; Choy, L.; Hagenbeek, T. J.; de Leon, G. P.; Chen, Y.; Finkle, D.; Venook, R.; Wu, X.; Ridgway, J.; Schahin-Reed, D.; Dow, G. J.; Shelton, A.; Stawicki, S.; Watts, R. J.; Zhang, J.; Choy, R.; Howard, P.; Kadyk, L.; Yan, M.; Zha, J.; Callahan, C. A.; Hymowitz, S. G.; Siebel, C. W. Therapeutic antibody targeting of individual Notch receptors. *Nature* **2010**, *464*, 1052−1057.

(25) Yoo, Y.; Lee, H.; Lee, H.; Lee, M.; Yang, S.; Hwang, A.; Kim, S.-i.; Park, J. Y.; Choo, J.; Kang, T.; Kim, B. Surfactant-Free Vapor-Phase Synthesis of Single-Crystalline Gold Nanoplates for Optimally Bioactive Surfaces. *Chem. Mater.* **2017**, *29*, 8747−8756.

DOI: 10.1021/acsami.8b13180
ACS Appl. Mater. Interfaces 2018, 10, 37829−37834